

RESEARCH

Open Access



Unraveling calcium dysregulation and autoimmunity in immune mediated rippling muscle disease

Samir R. Nath¹, Aneesha Dasgupta^{2,3}, Divyanshu Dubey¹, Eileen Kokesh¹, Grayson Beecher^{1,4}, Numrah Fadra⁵, Teerin Liewluck¹, Sean Pittock¹, Jason D. Doles^{2,3}, William Litchy¹ and Margherita Milone^{1*}

Abstract

Rippling Muscle Disease (RMD) is a rare skeletal myopathy characterized by abnormal muscular excitability manifesting with wave-like muscle contractions and percussion-induced muscle mounding. Hereditary RMD is associated with caveolin-3 or cavin-1 mutations. Recently, we identified cavin 4 autoantibodies as a biomarker of immune-mediated RMD (iRMD), though the underlying disease-mechanisms remain poorly understood. Transcriptomic studies were performed on muscle biopsies of 8 patients (5 males; 3 females; ages 26-to-80) with iRMD. Subsequent pathway analysis compared iRMD to human non-disease control and disease control (dermatomyositis) muscle samples. Transcriptomic studies demonstrated changes in key pathways of muscle contraction and development. All iRMD samples had significantly upregulated cavin-4 expression compared to controls, likely compensatory for autoantibody-mediated protein degradation. Proteins involved in muscle relaxation (including SERCA1, PMCA and PLN) were significantly increased in iRMD compared to controls. Comparison of iRMD to dermatomyositis transcriptomics demonstrated significant overlap in immune pathways, and the IL-6 signaling pathway was markedly increased in all iRMD patient muscle biopsies and increased in the majority of iRMD patients' serum. This study represents the first muscle transcriptomic analysis of iRMD patients and dissects underlying disease mechanisms. Increase of sarcolemmal and cellular calcium channels as well as PLN, an inhibitor of the SERCA pump for calcium into the sarcoplasm, likely alters the calcium dynamics in iRMD. These changes in crucial components of muscle relaxation may underlie rippling by altering calcium flux. Our findings provide crucial insights into the differential expression of genes regulating muscle relaxation and highlight potential disease pathomechanisms.

Keywords Immune mediated rippling muscle disease, Myopathy, Transcriptomics, Interleukin-6, Interferon

Introduction

Rippling muscle disease (RMD) is a rare disorder of muscle excitability which manifests with wave-like muscle contractions and percussion-induced rapid muscle contraction, often resulting in myalgia and muscle stiffness [1]. Muscle weakness occurs in a subset of patients [2–6]. RMD can be either hereditary (hRMD) or immune-mediated (iRMD). Mutations in two genes are so far known to cause hRMD, caveolin 3 (*CAV3*) and cavin-1 (*CAVIN1*). While caveolin-3 is a muscle-specific protein, cavin-1 is a caveolin-associated protein expressed in several tissues.

*Correspondence:

Margherita Milone
Milone.Margherita@mayo.edu

¹ Department of Neurology, Mayo Clinic, Rochester, MN 55905, USA

² Department of Biochemistry and Molecular Biology, Mayo Clinic, Rochester, MN 55905, USA

³ Department of Anatomy, Cell Biology, and Physiology, Indiana University School of Medicine, Indianapolis, IN 46202, USA

⁴ Division of Neurology, Department of Medicine, University of Alberta, Edmonton, AB T6G 2G3, Canada

⁵ Division of Computational Biology, Department of Quantitative Health Sciences Research, Mayo Clinic, Rochester, MN 55905, USA



© The Author(s) 2025, corrected publication 2025. **Open Access** This article is licensed under a Creative Commons Attribution-NonCommercial-NoDerivatives 4.0 International License, which permits any non-commercial use, sharing, distribution and reproduction in any medium or format, as long as you give appropriate credit to the original author(s) and the source, provide a link to the Creative Commons licence, and indicate if you modified the licensed material. You do not have permission under this licence to share adapted material derived from this article or parts of it. The images or other third party material in this article are included in the article's Creative Commons licence, unless indicated otherwise in a credit line to the material. If material is not included in the article's Creative Commons licence and your intended use is not permitted by statutory regulation or exceeds the permitted use, you will need to obtain permission directly from the copyright holder. To view a copy of this licence, visit <http://creativecommons.org/licenses/by-nc-nd/4.0/>.

CAV3-RMD demonstrates a wide spectrum of disease spanning from asymptomatic creatine kinase elevation to muscle weakness with predominant proximal or distal involvement [4, 5, 7–16]. *CAVIN1*-RMD is characterized by congenital generalized lipodystrophy and often associated with muscular dystrophy and additional extra-skeletal muscle manifestations [17–19].

Conversely, iRMD has an autoimmune etiology which is supported by the lack of pathogenic variants in *CAV3* and *CAVIN1*, clinical response to immunotherapy, post-immunotherapy restoration of caveolin-3 expression at the sarcolemma, coexistence of other autoimmune disorders, and occasional presence of inflammatory reaction in muscle [20–25]. Overlap syndrome with iRMD coexisting with seropositive myasthenia gravis and a positive response to immunotherapy has been also reported, supporting a role for autoimmunity in the driving of the rippling [26, 27]. Additionally, work from our group has identified autoantibodies against cavin-4, another caveolin-associated protein, as a specific biomarker of iRMD [25].

Proteins involved in both hRMD and iRMD are key structural components of the caveolae or play a crucial role in the formation of caveolae [18, 28–31]. These are invaginations of the sarcolemma with various functions, including regulation of endocytosis and exocytosis, sarcolemma repair, muscle development, and interaction with the T-tubule to mediate excitation contraction coupling (ECC) [25, 32, 33].

Recent studies have demonstrated a critical role for cavin-4 in muscle cell integrity, particularly in the development of T-tubules, a key component of ECC and the critical reservoir for calcium in skeletal muscle [30, 34]. The recent finding of cavin-4 autoantibodies in iRMD, accompanied by sarcolemmal cavin-4 loss with a mosaic pattern matching caveolin-3 loss in muscle, has led to the hypothesis that autoimmune responses disrupting key proteins involved in skeletal muscle excitation and relaxation underlie disease pathogenesis in iRMD.

To explore this hypothesis, we conducted transcriptomic analysis of skeletal muscle tissue from iRMD patients. When compared to non-disease controls, several key genes involved in muscle relaxation were altered in iRMD, and such findings were confirmed by immunohistochemical studies on patients' skeletal muscle tissue. Pathways of skeletal muscle development and differentiation were also significantly altered in iRMD. Additionally, investigation of autoimmunity pathways revealed a unique signature of iRMD with a robust induction of the interleukin-6 (IL-6) pathway in the absence of interferon one or two induction. This study lays the foundation for the development of targeted therapies by elucidating critical pathogenic alterations at the core of iRMD.

Methods

Patients

The study was approved by the Mayo Clinic Institutional Review Board (IRB#18–010637). Patients were identified by searching Mayo Clinic medical records and the muscle pathology laboratory database between 01/2000 through 08/02/2021. All patients included were evaluated by a neuromuscular specialist and diagnosed with iRMD based on: (1) Percussion and/or stretch induced rolling movements across a muscle or muscle group (rippling), (2) Percussion induced rapid muscle contraction with or without percussion induced muscle-mounding, (3) Lack of fibrillation, fasciculation and motor unit action potentials detected by needle electromyography (EMG) during the muscle rippling or mounding, (4) Absence of pathogenic variants in *CAV3* and *CAVIN1* by DNA sequencing, (5) Presence of cavin-4 autoantibodies in all but one patient (tested after receiving IVIG treatment) as previously published [25].

RNA isolation and sequencing

RNA was extracted from muscle tissue of eight iRMD patients using the AllPrep Universal Kit. Total RNA was quantified using the Quant-iT™ RiboGreen RNA Assay Kit and normalized to 5 ng/μl. Subsequently, 2 μL of ERCC controls were spiked into each sample. 325 ng per sample was transferred into library preparation using an automated variant of the Illumina TruSeq™ Stranded mRNA Sample Preparation Kit. Oligo dT beads were used to select mRNA from the total RNA sample, followed by heat fragmentation and cDNA synthesis from the RNA template. cDNA then underwent dual-indexed library preparation: 'A' base addition, adapter ligation using P7 adapters, and PCR enrichment using P5 adapters. After enrichment the libraries were quantified using Quant-iT PicoGreen at a 1:200 dilution. Samples were normalized to 5 ng/μL, and the set was pooled and quantified using qPCR. All pipetting was done by either Agilent Bravo or Hamilton Starlet.

Pooled libraries were normalized to 2 nM and denatured using 0.1 N NaOH prior to sequencing. Flowcell cluster amplification and sequencing were performed according to the manufacturer's protocols using the NovaSeq 6000. Each run consisted of 101 bp paired-end reads with an eight-base index barcode. Muscle RNA extraction and sequencing was performed in a commercial laboratory (Broad Institute, Massachusetts Institute of Technology, Cambridge, MA).

The raw reads for the eight iRMD muscle biopsies, as well as eight publicly available GTex non-disease control cohort samples and previously published NIH non-disease control and dermatomyositis cohorts were aligned using the MAPR-seq pipeline (v3.1.0) and hg38 reference

genome [25, 35, 36]. Alignment was achieved using the STAR aligner and counts were generated using featureCounts [37]. Variants were called using the RVBoost module from MAPR-seq. Gene and exon expression quantification was performed using the Subread package to obtain both raw and normalized (FPKM—Fragments Per Kilobase per Million mapped reads) reads [38]. FASTQC, MultiQC, and RSEQC tools were used for comprehensive quality control assessment of the aligned reads. Principle Component Analysis (PCA) analysis was performed to ensure there were no outliers and to ensure fidelity in each group. Differential expression was determined using EdgeR [39]. Pathway analysis was performed using Gene Ontology (GO-Term) analysis [40, 41]. False discovery rate was set as $P_{\text{adj}} < 0.05$.

Immunohistochemistry and image acquisition

Muscle biopsies from the eight patients with iRMD from the RNA sequencing cohort underwent confirmatory immunohistochemistry studies. Three pathologically normal muscle biopsies from patients with normal creatine kinase and without a diagnosis of muscle disease were used as non-disease control tissue.

Samples were cut at 6 μm for fluorescent immunohistochemistry and fixed in -20°C methanol for 4 min prior to staining. Non-specific binding was blocked for 20 min in 10% normal donkey serum (Jackson ImmunoResearch, #017-000-121). Sections were incubated at room temperature for 1 h in each primary antibody, followed by three 5-min rinses in 1X PBS buffer (ScyTek, PBD999). Sections were then labeled with the corresponding secondary antibodies for 1 h at room temperature, then rinsed in running distilled water for 5 min before mounting with Vectashield antifade mounting medium (Vector Laboratories, H-1000-10).

The following primary antibodies were used for immunohistochemical studies: CACNA1S (1:200 ThermoFisher, MA3-290), SERCA1 (1:100, Abcam, ab2819), PMCA (1:50, ThermoFisher, MA3-914), Phospholamban (1:200, ThermoFisher, MA3-922), TOMM20 (1:250, Santa Cruz, sc-17764), RYR1 (1:100, Cell Signaling, #8153). The following secondary antibodies were used for labeling: FITC Affinipure Donkey Anti-Mouse IgG (1:200, Jackson ImmunoResearch, #715-095-150) and TRITC Affinipure Donkey Anti-Rabbit (1:200, Jackson ImmunoResearch, #711-025-152).

Confocal images were captured using an LSM 910 Zeiss microscope.

Quantification and statistical analysis

All images were quantified using Cell Profiler (Broad Institute) [23]. Heatmaps and data visualizations were

generated using matplotlib and python. For immunofluorescent studies, statistical analysis was performed in Graphpad Prism using two-tailed unpaired Student's t-test. $\alpha < 0.05$ was set as the threshold for significance. A schematic illustration figure was created using BioRender.

Results

Upregulation of CAV3, CAVIN1 and CAVIN4 in iRMD skeletal muscle biopsies

To define the transcriptomic profile of iRMD skeletal muscle, RNA sequencing was performed on muscle biopsies from a cohort of eight iRMD patients (Supplemental Table 1). Findings were compared to those from a cohort of previously published non-disease control skeletal muscle biopsies [35]. Hierarchical clustering and PCA analysis showed clear separation between iRMD patient muscle biopsies and non-disease controls (Supplemental Fig. 1 and 2). When compared to non-disease controls, 8640 genes displayed significantly ($p_{\text{adj}} < 0.05$, $\text{FC} > 1.5$) altered expression in iRMD patient muscle biopsies. 4577 genes showed increased expression in iRMD muscle and 4063 were diminished in expression.

As previous studies have demonstrated acquired patchy loss of caveolin-3 in iRMD skeletal muscle and because hRMD is caused by mutations in *CAV3* or *CAVIN1*, we first determined whether expression of these genes is altered in iRMD [11, 15, 20, 42]. Compared to non-disease controls, iRMD patient muscle demonstrated significantly increased mRNA expression of *CAV3* and *CAVIN1* (Fig. 1).

Given the recent discovery of anti-cavin-4 auto-antibodies and patchy loss of sarcolemmal cavin-4 in iRMD, we also sought to determine if *CAVIN4* expression was altered in iRMD skeletal muscle [25]. Similarly to *CAV3*, *CAVIN4* expression also was significantly increased in iRMD skeletal muscle samples compared to non-disease control (Fig. 1).

Further, when iRMD patient muscle biopsies were compared to an independent GTEX cohort of non-disease controls, *CAVIN4* and *CAV3* remained greater than five-fold upregulated, although *CAVIN1* was not differentially expressed (Supplemental Table 2).

Pathways of Skeletal Muscle Function and Calcium Ion Signaling are altered in iRMD patient skeletal muscle

We next sought to determine whether pathways of skeletal muscle function were significantly altered in iRMD patient muscle biopsies compared to non-disease controls.

Gene Ontology pathway analysis (GO-Term) was performed on all genes with significantly altered expression

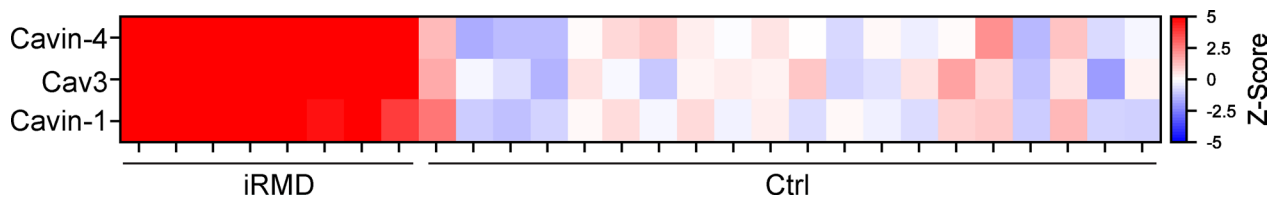


Fig. 1 Proteins implicated in hereditary RMD (hRMD) and immune mediated RMD (iRMD) display increased expression in iRMD. RNA was isolated from iRMD skeletal muscle biopsies and sequenced, and compared against previously published non-disease controls (Ctrl). Z-scores for *CAV3*, *CAVIN1*, and *CAVIN4* were calculated from expression levels across samples. iRMD=immune mediated rippling muscle disease, Ctrl=non-disease control biopsies

between iRMD and non-disease control. Several pathways involved in skeletal muscle development or differentiation were identified as enriched (Fig. 2A). Notably, these pathways included *CAV3* and *CAVIN4*, identifying these genes as key players of skeletal muscle alteration in iRMD (Fig. 2B, and Supplemental Table 3). Differential pathways showed relatively equal splits between genes increased and decreased in expression in iRMD patient muscle biopsies (Fig. 2B, C). Further, pathways of both T-tubule organization as well as regulation of cardiac muscle contraction by calcium ion signaling were significantly and differentially expressed in iRMD skeletal muscle compared to non-disease controls (Fig. 2A, Supplemental Table 3).

Additionally, bridging integrator 1 (*BINI*), which encodes a cavin-4 interacting protein concentrated at T-tubules known to cause a centronuclear myopathy when mutated, is also dysregulated in iRMD (Supplemental Table 4) [30, 43]. Such findings support a critical role for calcium dysregulation underlying the phenomenon of rippling (Fig. 2A, C).

Channels of muscle excitation and mitochondria remain unchanged at the protein level in iRMD muscle

Given iRMD is characterized by wave-like muscle contractions and stretch induced muscle mounding, we aimed to determine whether changes in expression of genes involved in muscle excitation or relaxation occur in iRMD skeletal muscle. This was performed by utilizing the transcriptomics data set and immunofluorescence staining quantification.

The pathways of muscle excitation and relaxation have been previously well characterized. In brief, calcium initially enters the cytoplasm via membrane

calcium channel Cav1.1 (*CACNA1S*). This influx of calcium triggers ryanodine receptor 1 (*Ryr1*) to release calcium from the sarcoplasmic reticulum [44, 45]. To allow relaxation, calcium is pumped back into the extracellular space by the plasma membrane Ca^{++} ATPase (PMCA) and into the sarcoplasmic reticulum by SarcoEndoplasmic Reticulum Calcium ATPase (SERCA) [45]. Phospholamban (PLN) has been demonstrated to inhibit the SERCA activity allosterically, causing significant reduction in pump affinity for calcium and decreasing ATPase activity of SERCA [46, 47].

Compared to non-disease controls, iRMD muscle shows a significant increase in *CACNA1S* expression (5.38 fold increase, $p=7.5E-42$), while *RYR1* expression was not significantly different (1.22 fold increase, $p=0.178$). We also assessed and compared protein levels of *CACNA1S* and *RYR1* between iRMD skeletal muscle and non-disease controls and found no significant difference between *CACNA1S* and *RYR1* immunofluorescence quantification (Fig. 3). Given ATP is produced by mitochondria in close proximity to T-tubules forming mitochondrial associated membranes with the structure, and that the pattern of colocalization is disrupted in other myopathic disorders, we also analyzed *TOMM20* RNA expression and protein level. Though *TOMM20* expression was increased, there was no change in the protein level by immunohistochemical quantification or its colocalization with *RYR1* in iRMD compared to controls (Fig. 3).

(See figure on next page.)

Fig. 2 iRMD Skeletal Muscle shows alterations in pathways of calcium regulation, muscle contraction, muscle development, and muscle differentiation. **A** Bubble plot of GO Term analysis of differentially expressed genes in iRMD skeletal muscle compared to healthy controls shows pathways of muscle t-tubules, calcium regulation, muscle differentiation, and muscle development are significantly altered in iRMD. **B** Heatmap of differentially expressed genes in muscle organ development GO-Term. **C** Heatmap of differentially expressed genes in regulation of cardiac muscle contraction by calcium ion signaling GO-Term

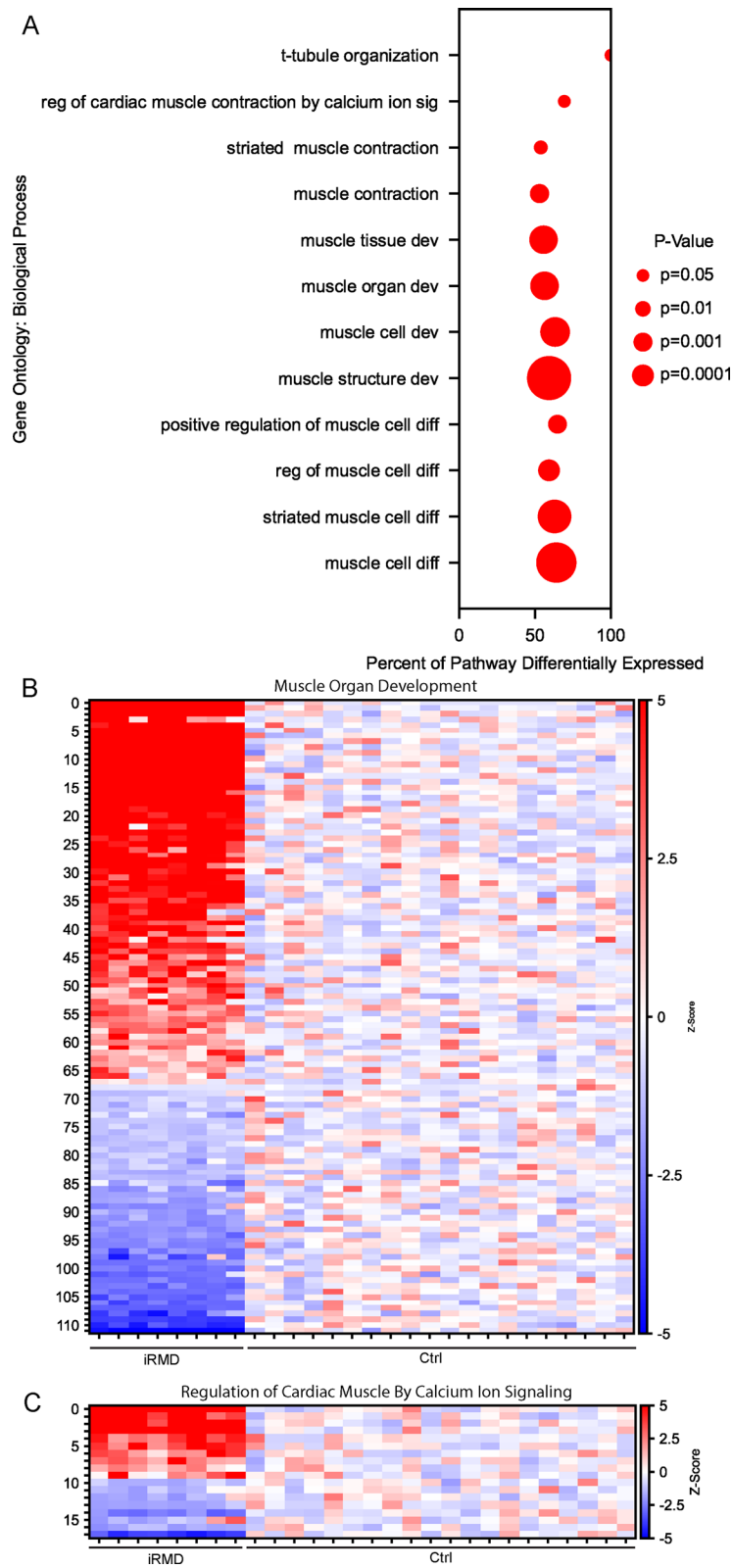


Fig. 2 (See legend on previous page.)

Changes in key muscle relaxation gene expression occur at the RNA and protein level in iRMD muscle

Next, we investigated whether expression of genes involved in muscle relaxation was altered in iRMD. SERCA1 (1.39 fold, $p=0.022$), PMCA (2.12 fold, $p=1.12E-10$), and PLN (33.96 fold, $p=5.5E-146$) all showed a statistically significant increase in expression. SERCA1 did not meet 1.5 fold change criteria (Fig. 4A), though it did attain a statistically significant p_{adj} (Fig. 4A). Immunofluorescence staining further demonstrated that protein level changes mirror expression level changes of PLN, PMCA, and SERCA1 in iRMD muscle (Fig. 4B and Supplemental Fig. 3). Though PLN RNA expression has been shown to be a marker of type 1 fibers, several other markers of type 1 fibers were not increased in expression in our RNA-seq dataset in iRMD muscle biopsies (Supplemental Table 5), suggesting that induction of PLN is not due to changes in predominant fiber type or fiber type shift [48].

Interferon pathways are not significantly induced in iRMD compared to healthy controls

Our group has recently demonstrated that auto-antibodies against cavin-4 are a specific biomarker of iRMD [25]. Hence, we next examined whether activation of pathways of autoimmunity observed in autoimmune myopathies are activated in iRMD. Interferon alpha has been suggested to play a key role in dermatomyositis (DM) where dendritic cells produce an abundance of interferon alpha and the interferon pathway is expressed at high levels in muscle biopsies [49, 50]. Utilizing previously described upregulated markers of type 1 interferon activation in dermatomyositis, we evaluated whether type 1 interferon-inducible gene overexpression represented a significant hallmark of iRMD [49]. In iRMD compared to non-disease controls, only one of these genes showed significantly increased expression, *RSAD2*, with many genes showing significantly decreased expression, including *ISG15*, *IFI6*, *MX1*, *MX2*, *OAS1*, *IRF9*, and *IFI35* (Fig. 5A).

Given the lack of robust interferon type-1 induction, we next evaluated whether type-2 interferon signaling was activated in iRMD. Previous literature identified increased expression of interferon type-2-inducible genes in dermatomyositis, inclusion body myositis,

anti-synthetase syndrome, and more recently in immune checkpoint inhibitor-dermatomyositis and myositis with associated myocarditis [49, 51]. In these disorders, specific markers of IFN2 induction included *IFI30*, *GBP2*, *GBP1*, *PSMB8* [49, 51]. We evaluated expression of these genes in iRMD compared to non-disease controls and found that only GBP2 showed significantly increased expression, while *IFI 30*, *GBP1*, and *PSMB8* were unchanged, suggesting that iRMD lacks induction of the type-2 interferon pathway as well (Fig. 5B).

The IL-6 pathway is induced in iRMD muscle

Induction of the IL-6 pathway was recently shown in patients with various subtypes of immune checkpoint inhibitor myositis [51]. IL-6 also serves as a myokine with multiple pro- and anti-inflammatory properties [52]. To evaluate whether the IL-6 pathway is induced in iRMD, we initially compiled a list of genes known to be part of the IL-6 mediated signaling pathway by gene ontology analysis (GO: 0070102) [41, 51]. When filtered by genes detected in our data set, 14 genes comprised the list of IL-6 inducible genes (*IL-6ST*, *IL-6R*, *FER*, *CTR9*, *SRC*, *SPI1*, *SMAD4*, *STAT3*, *CEBPA*, *YAP1*, *JAK1*, *GAB1*, *JAK2*, and *ZCCHC11*). All of these genes were significantly differentially expressed in iRMD patients' muscle biopsies compared to non-disease controls except for *SMAD4* and *ZCCHC11* ($p=0.038$ by hypergeometric test), demonstrating significant induction of the IL-6 pathway (Fig. 6). Further, when patient serum was analyzed, four out of six iRMD patients showed increased IL-6 protein levels, with half of patients showing IL-6 levels above the 99th percentile of the normal range (Supplemental Table 6).

Given the identification of IL-6 pathway activation through transcriptomic analysis of iRMD muscle as well as the recent finding of cavin-4 antibodies in iRMD, we next sought to compare changes in gene expression in iRMD to an autoimmune inflammatory myopathy. To accomplish this, a previously published transcriptomics dataset of dermatomyositis was reanalyzed along the same pipeline and to the same control group to compare expression level changes in dermatomyositis to iRMD [35]. Genes which were differentially expressed in both iRMD and dermatomyositis were analyzed with GO-Term analysis. Pathways

(See figure on next page.)

Fig. 3 CACNA1S, RYR1 and TOM20 expression level and immunofluorescence in iRMD compared to non-disease controls. **A** Heatmap of CACNA1S expression in transcriptomic data set of iRMD compared to non-disease controls. **B** Immunofluorescence staining of CACNA1S showed no significant difference in protein level. **C** Significantly increased expression was found for *TOMM20* but not *RYR1* using RNA sequencing transcriptomic analysis on iRMD patient's skeletal muscle biopsies compared to non-disease controls. **D** Immunofluorescence staining of RYR1 and TOMM20 demonstrated no significant difference in expression or colocalization in iRMD patient's compared to non-disease controls. Scale bar = 10um., ns = not significant

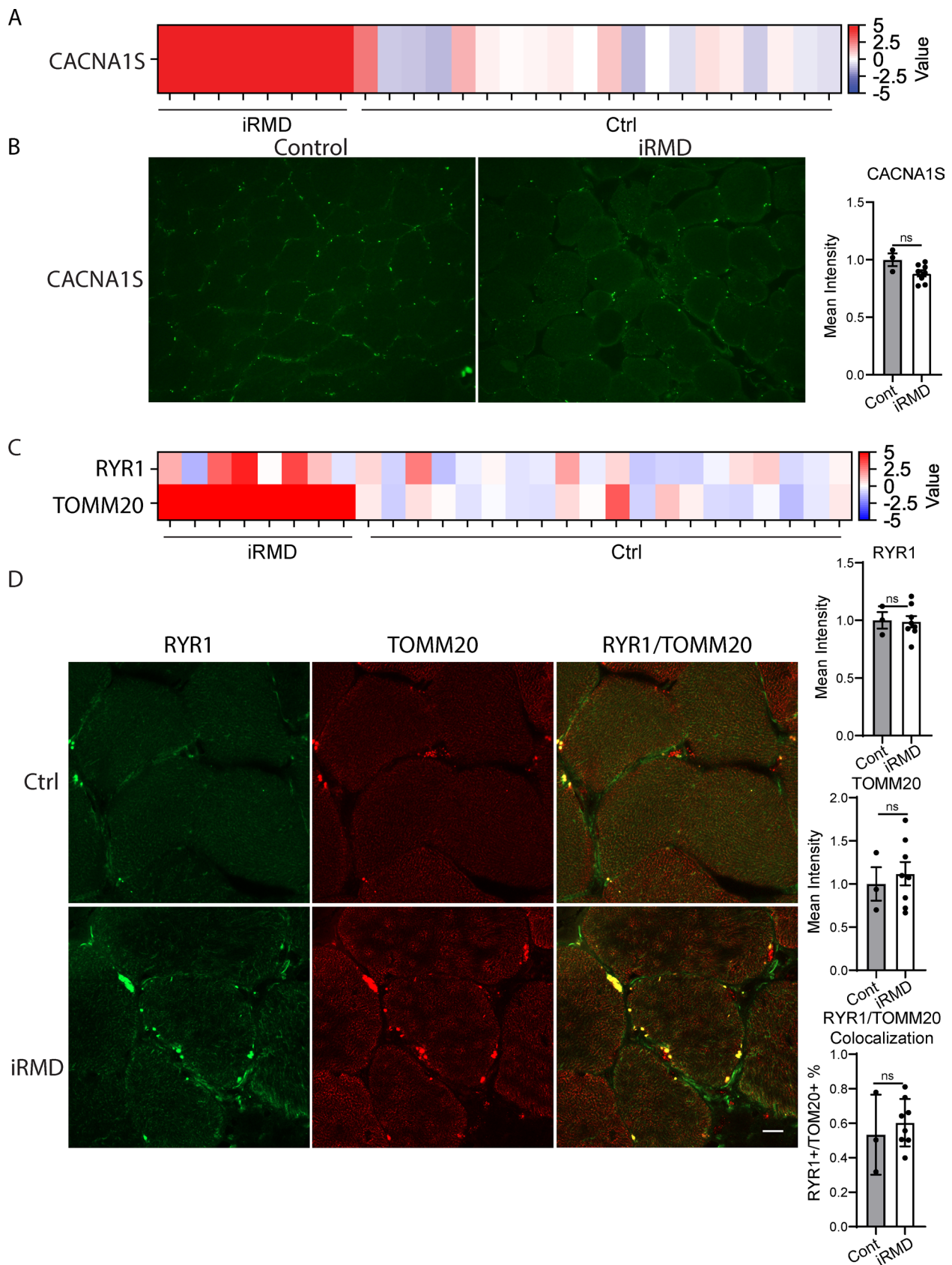


Fig. 3 (See legend on previous page.)

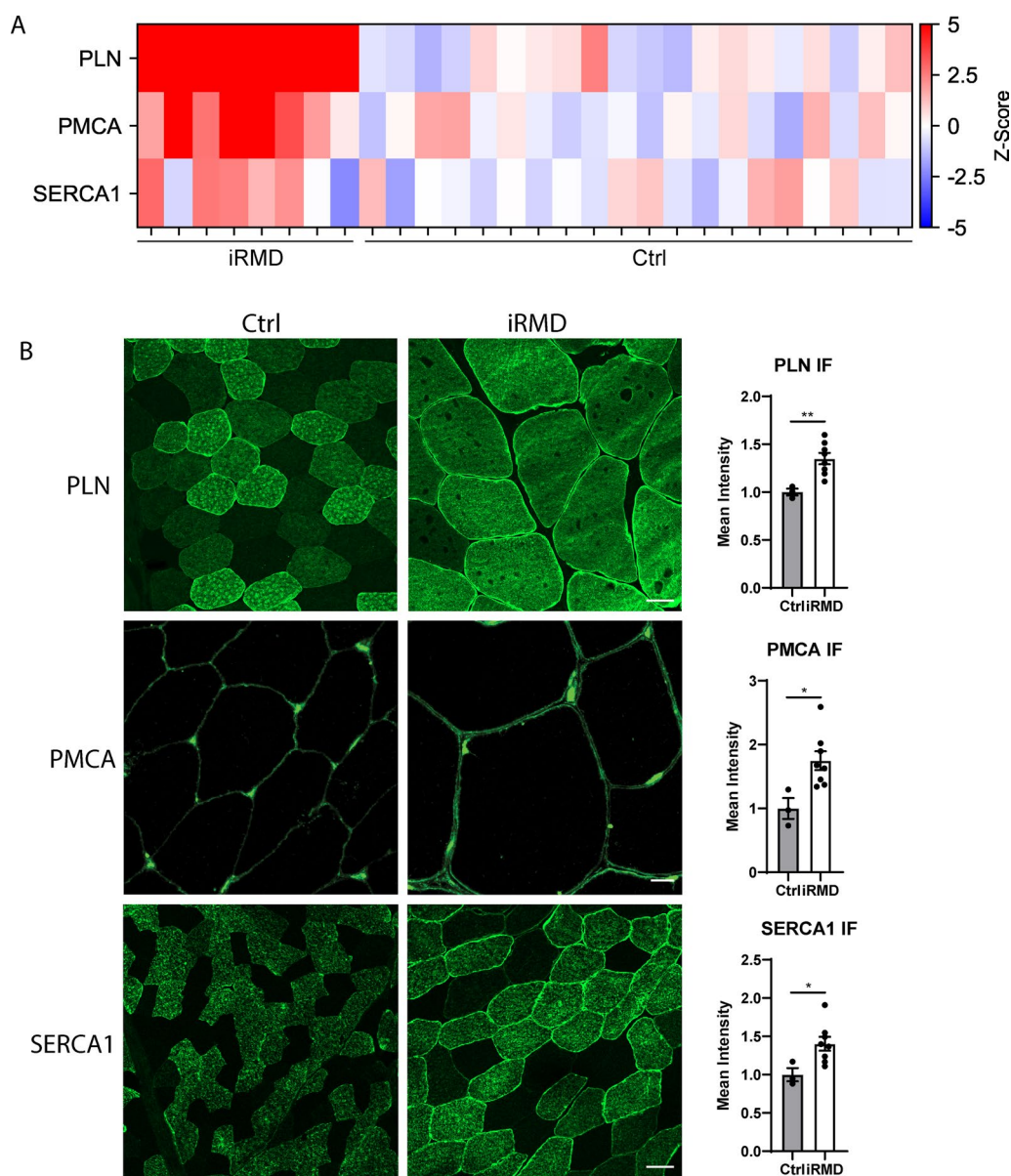


Fig. 4 Skeletal muscle from iRMD patients shows altered expression and protein level of critical regulators of calcium flux and muscle relaxation. **A** Heatmap showing expression of *PLN*, *PMCA*, and *SERCA1* in iRMD patient skeletal muscle biopsies compared to non-disease controls. **B** Immunofluorescent staining of iRMD skeletal muscle compared to non-disease controls. * $p < 0.05$, ** $p < 0.01$. Scale bars: PLN = 50um, PMCA = 10um, SERCA1 = 50um

involved in immune response, immune activation, or signaling pathways of immune activity were significantly enriched amongst overlapping genes between iRMD and DM (Supplemental Fig. 4). These findings likely represent overlapping nonspecific pathways of autoimmune myopathies supporting the role of immune activation in iRMD.

Discussion

This study represents the first transcriptomic analysis performed in skeletal muscle of iRMD patients and sheds light on its so far poorly understood pathogenesis (Fig. 7). We demonstrate two key findings in iRMD muscle: (1) Changes in RNA transcripts and related protein expression of key genes involved in muscle relaxation which could underlie the rippling phenomenon (Figs. 1, 2, 3, 4); (2) A robust induction of immune pathways with a

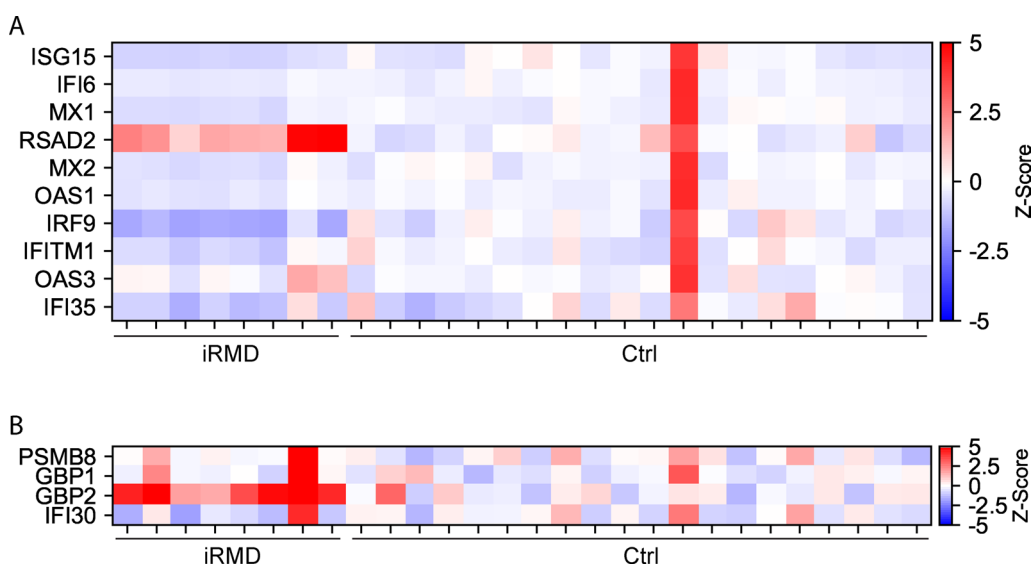


Fig. 5 Interferon type-1 and Interferon type-2 pathways are not induced in iRMD skeletal muscle biopsies. **A** Heatmap of expression z-scores of Interferon type-1 inducible genes in iRMD skeletal muscle biopsies compared to non-disease controls. **B** Heatmap of expression z-scores of Interferon type-2 inducible genes in iRMD skeletal muscle biopsies compared to non-disease controls

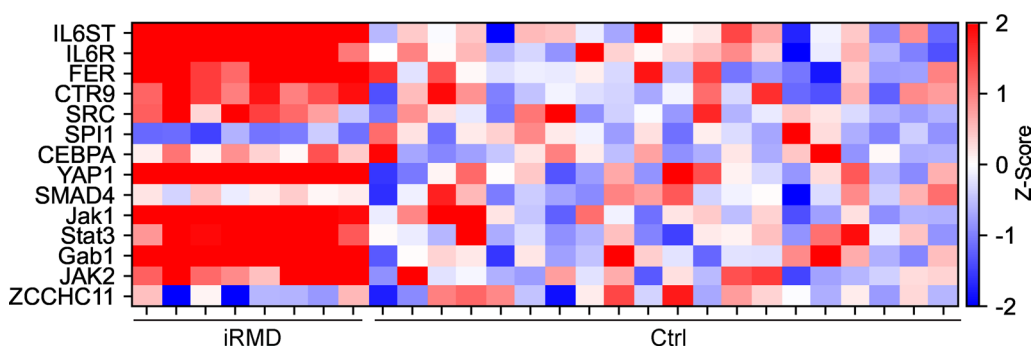


Fig. 6 The IL-6 pathway is activated in iRMD. Heatmap of IL-6 inducible genes in iRMD skeletal muscle biopsies compared to non-disease controls

unique signature with lack of induction of the IFN1 and IFN2 pathways and robust induction of the IL6 pathway (Figs. 5, 6, Supplemental Fig. 4).

Our findings suggest that the early events in muscle contraction that involve the nicotinic acetylcholine receptor, Cav1.1 (*CACNA1S*) and RYR1 are unchanged at the protein level, indicating adequate compensation in skeletal muscle of iRMD patients (Fig. 3). At the transcript (mRNA) level, however, *CACNA1S*, as well as *TOMM20*, are both increased, and this may represent an attempted compensatory response to preserve the machinery involved in muscle excitation.

Conversely, muscle relaxation is expected to be compromised as suggested by the increased *PLN*, *PMCA*, and *SERCA* at both the mRNA and protein level. Notably, *PLN* is elevated nearly 30-fold at the RNA level (Fig. 4). In skeletal muscle, *PLN* overexpression can impair *SERCA* activity and alter muscle contractility and relaxation [53,

54]. In cardiac muscle, *PLN* regulates cytosolic calcium by modulating *SERCA* affinity for calcium and inhibiting its ATPase activity, thereby slowing calcium reuptake into the sarcoplasmic reticulum [47, 55, 56]. Therefore, the increased *PLN* expression (at both the mRNA and protein level) in iRMD could play a crucial role in driving impaired muscle relaxation. It is likely that the increase in *PLN* RNA and protein level plays a key role in maintaining high levels of cytosolic calcium in iRMD and this in turn could lead to prolonged or recurrent sarcomeric contraction. *SERCA* is critical for terminating muscle contraction by pumping calcium back into the sarcoplasmic reticulum [44]. The finding of increased *SERCA* level could represent a compensatory response to its suppressed activity by *PLN*. The increased *PMCA* expression, which pumps calcium back into the extracellular space and is equally relevant in stopping muscle contraction, could constitute an attempt to restore intracellular

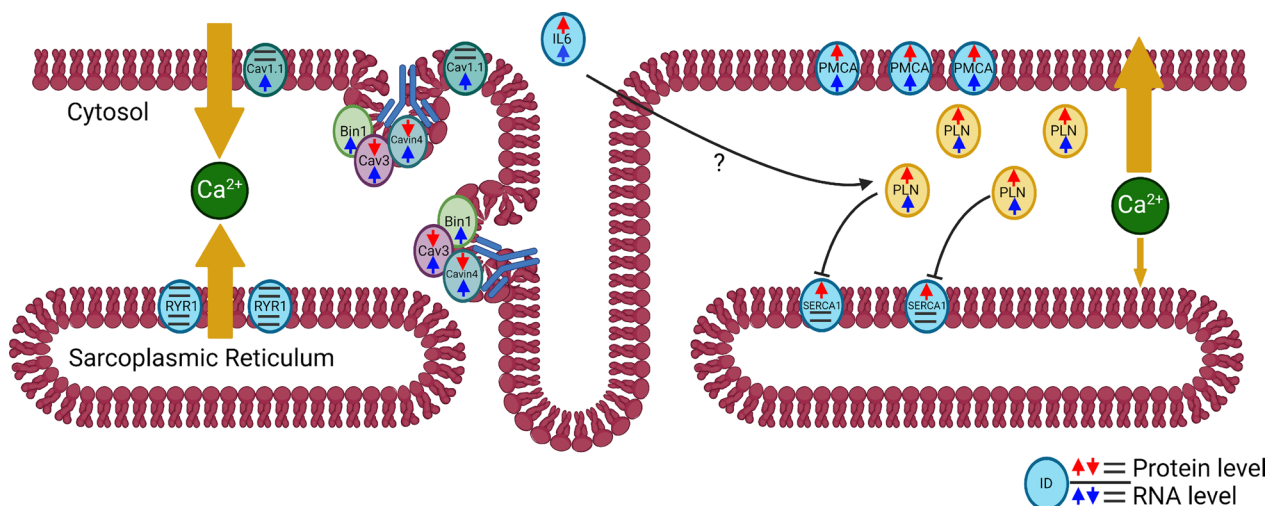


Fig. 7 Schematic illustration of pathophysiologic changes in iRMD. Left: Calcium enters the skeletal muscle cytosol through Cav1.1 and Ryr1. In iRMD, antibodies bind to Cavin-4 at caveolae. IL6 expression and protein level are increased. Right: SERCA1 and PMCA, proteins involved in muscle relaxation, are increased at the protein level. PLN, an inhibitor of SERCA1, is dramatically increased in expression in iRMD skeletal muscle. This may interfere with the ability of calcium to return to the sarcoplasmic reticulum, instead exiting through PMCA to the extracellular space. Blue arrows: RNA expression level. Red arrows: Protein expression level

calcium concentration and normal muscle contractility. All this would support a defect in muscle relaxation underlying the muscle rippling and mounding that characterize iRMD. Of relevance, despite the expression of both PLN and cavin-4 in cardiac muscle, iRMD patients had no cardiac symptoms and those who underwent cardiac studies showed minimal electrocardiographic abnormalities, though not all patients underwent comprehensive heart investigations [25].

Muscle of iRMD patients also shows increased transcript levels of caveolin-3 and cavin-4, both of which are involved in iRMD. Indeed, mosaic loss of caveolin-3 with corresponding loss of cavin-4 is the immunohistopathological hallmark of iRMD while cavin-4 autoantibodies are its serological biomarker and likely responsible for the cavin-4 depletion [25]. Interestingly, muscle levels of caveolin-3 and cavin-4 transcripts are increased (Fig. 1). This may represent a compensatory increase in mRNA transcripts in response to rapid degradation of the proteins, although the possibility of a translational block cannot be excluded. Considering that transcriptomic analysis was performed on bulk RNA, one cannot establish with certainty if the increased transcript levels of caveolin-3 and cavin-4 occurs diffusely in muscle, only in muscle fibers with reduced expression of these specific proteins or in normal muscle fibers. Based, however, on our previous estimate that approximately 80% of fibers in

a muscle biopsy of iRMD patients show loss of caveolin-3 and cavin-4 [25], it is likely that the increased *CAV3* and *CAVIN4* transcripts occur in muscle fibers with loss of these specific proteins.

BIN1, which encodes a protein interacting with cavin-4, is also increased in expression (Supplemental Table 4). Previous upregulation of *BIN1* was observed in response to cavin-4 loss and suspected to represent a compensatory mechanism [30]. Cavin-4, caveolin-3 and bin1 are all expressed on the T-tubule membrane. Cavin-4 is intimately linked to caveolin 3 in the caveolae along T-tubules [57], and directly interacts with bin1 [30]. Cavin-4 is important in maintaining the structural and functional integrity of the T-tubules and its loss leads to T-tubule fragmentation and impaired calcium release [30]. Bin1 was suggested to drive T-tubule formation.

We hypothesize that a breakdown in the T-tubule-SERCA interactions in iRMD results in a decreased ability to pump calcium out of the cytosol leading to a failure of relaxation at the site of stimulation with propagation to surrounding areas.

This study also identifies induction of immune activation pathways supporting the role of autoimmunity in disease pathogenesis, which is in line with the detection of cavin-4 autoantibodies in serum and complement membrane attack complex (MAC) on non-necrotic muscle fibers in iRMD [25]. Here, we expand the

understanding of iRMD pathogenesis by illustrating the complex interplay between skeletal muscle gene expression and immune system activation. iRMD is characterized by a unique immunologic signature. It did not show induction of the IFN1 and IFN2 pathways as is characteristic of certain immune-mediated myopathies, such as dermatomyositis (Fig. 5) and to a lesser degree immune mediated necrotizing myopathy (IMNM) [49]. We identified the upregulation of IL6 in iRMD, a myokine with diverse roles in immune modulation and skeletal muscle physiology [52]. IL6 secretion exponentially increases with physical activity and is controlled at transcription level [52]. In iRMD, IL6 overexpression may reflect continuous muscle activity secondary to a defect in muscle relaxation, a marker of immune response or a combination of both. IL6 is upregulated in congenital myotonic dystrophy, another disorder of muscle contractility, supporting a role for IL6 induction in the pathogenesis of disorders with aberrant muscle contraction [58]. Further, IL6 is upregulated in immune checkpoint inhibitor-myositis [51]. Contrary to this type of myositis, where many biopsies showed an inflammatory reaction most iRMD muscle specimens revealed no inflammation [25]. Given IL-6 production can occur in response to muscle contraction, its role in immune response and its upregulation in iRMD, available IL6 receptor inhibitors and other drugs targeting the IL6 pathway could represent an additional novel therapeutic tool in iRMD.

There are several limitations to this study. The number of biopsy samples is limited and expansion of transcriptomics studies to more patient specimens could help to better dissect disease mechanisms and validate findings. Single-nuclei RNA sequencing only in muscle fibers depleted of caveolin-3 and cavin-4 could provide a more precise profile of gene expression changes. Future studies focusing on longitudinal analysis of gene expression could inform the progression of these molecular changes and their relationship with clinical outcomes. Additionally, investigating the functional consequences of these gene expression changes in muscle cells could provide insights into the molecular mechanisms driving iRMD symptoms.

Despite these limitations, this study provides insight into the mechanisms leading to the electrically silent rippling phenomenon and lays the groundwork for targeted therapeutic approaches that can modulate the identified pathways, offering new avenues for treatment in iRMD and similar disorders.

Abbreviations

iRMD	Immune mediated rippling muscle disease
DM2	Dermatomyositis
IMNM	Immune mediated necrotizing myopathy
hRMD	Hereditary rippling muscle disease

Supplementary Information

The online version contains supplementary material available at <https://doi.org/10.1186/s40478-025-01926-z>.

Additional file 1.

Acknowledgements

We thank Asha Nair, PhD, bioinformatician, and Attila Kumanovics, MD, Department of Laboratory Medicine and Pathology, Mayo Clinic, Rochester, MN, for their initial input on data analysis. A schematic illustration figure was created using BioRender [59].

Author contributions

SRN, GB, JD, WL, and MM planned experiments. SRN, AD, DD, EK, GB, and NF performed experiments. SRN, AD, DD, EK, GB, NF, TL, SP, JDD, WL, and MM interpreted data and critically reviewed the manuscript. SRN and MM wrote the manuscript.

Funding

Department of Neurology through Small Grants Program Award and Discretionary Fund (to M.M.), and CCaTS Team Science Pilot Award (to J.D.D. and M.M.), Mayo Clinic, Rochester, MN, 55905.

Data availability

Sequence data supporting the findings of this study have been deposited in the GEO database under accession GSE280931.

Declarations

Ethics approval and consent to participate

This study was approved by the Mayo Clinic Institutional Review Board (IRB#18-010637).

Consent for publication

All authors have reviewed and approved the final version of the manuscript and consent to its publication in *Acta Neuropathologica Communications*. The study was approved by the Mayo Clinic Institutional Review Board (IRB#18-010637).

Competing interests

MM has received personal compensation for serving on a Scientific Advisory or Data Safety Monitoring board for Argenx on an unrelated topic and for serving as an Associate Editor for Neurology Genetics, AAN. SP has received personal compensation for consulting roles with Genentech, Sage Therapeutics, Prime Therapeutics, UCB, Roche/Genentech, and Arialyis Therapeutics, as well as for serving on a Scientific Advisory or Data Safety Monitoring board for UCB, Inc., Genentech, and F. Hoffman/LaRoche, for advisory work with Hoffman/LaRoche AG and Alexion, for consulting roles with Astellas, Alexion, MedImmune/Viela Bio, and Roche/Genentech. His institution has received research support from Grifols, NIH, Viela Bio/MedImmune/Horizon, Alexion Pharmaceuticals, F. Hoffman/LaRoche/Genentech, NovelMed, and AstraZeneca. SP holds intellectual property interests in healthcare-related discoveries and technologies. D.D. has consulted for UCB, Immunovant, Argenx, Arialyis and Astellas pharmaceuticals. All compensation for consulting activities is paid directly to Mayo Clinic. He is a named inventor on filed patent that relates to KLHL11 as marker of autoimmunity and germ cell tumor. He has patents pending for LUZP4-IgG, cavin-4-IgG and SKOR2 IgG as markers of neurological autoimmunity. He has received funding from the DOD (CA210208 & PR220430), David J. Tomassoni ALS Research Grant Program and UCB.

Received: 10 November 2024 Accepted: 6 January 2025
Published: 16 January 2025

References

- Schulte-Mattler WJ et al (2005) Immune-mediated rippling muscle disease. *Neurology* 64(2):364–367
- McNally EM et al (1998) Caveolin-3 in muscular dystrophy. *Hum Mol Genet* 7(5):871–877
- Muller JS et al (2006) Novel splice site mutation in the caveolin-3 gene leading to autosomal recessive limb girdle muscular dystrophy. *Neuromuscul Disord* 16(7):432–436
- Berling E et al (2023) Caveolinopathy: Clinical, histological, and muscle imaging features and follow-up in a multicenter retrospective cohort. *Eur J Neurol* 30(8):2506–2517
- Fulizio L et al (2005) Molecular and muscle pathology in a series of caveolinopathy patients. *Hum Mutat* 25(1):82–89
- Minetti C et al (1998) Mutations in the caveolin-3 gene cause autosomal dominant limb-girdle muscular dystrophy. *Nat Genet* 18(4):365–368
- Ueyama H et al (2007) Novel homozygous mutation of the caveolin-3 gene in rippling muscle disease with extraocular muscle paresis. *Neuromuscul Disord* 17(7):558–561
- Traverso M et al (2008) Truncation of caveolin-3 causes autosomal-recessive rippling muscle disease. *J Neurol Neurosurg Psychiatry* 79(6):735–737
- Vorgerd M et al (2001) A sporadic case of rippling muscle disease caused by a de novo caveolin-3 mutation. *Neurology* 57(12):2273–2277
- Bae JS et al (2007) A novel in-frame deletion in the CAV3 gene in a Korean patient with rippling muscle disease. *J Neurol Sci* 260(1–2):275–278
- Kubisch C et al (2005) Autosomal recessive rippling muscle disease with homozygous CAV3 mutations. *Ann Neurol* 57(2):303–304
- Lorenzoni PJ et al (2007) A novel missense mutation in the caveolin-3 gene in rippling muscle disease. *Muscle Nerve* 36(2):258–260
- Madrid RE, Kubisch C, Hays AP (2005) Early-onset toe walking in rippling muscle disease due to a new caveolin-3 gene mutation. *Neurology* 65(8):1301–1303
- Schara U et al (2002) Rippling muscle disease in childhood. *J Child Neurol* 17(7):483–490
- Carbone I et al (2000) Mutation in the CAV3 gene causes partial caveolin-3 deficiency and hyperCKemia. *Neurology* 54(6):1373–1376
- Milone M et al (2012) Myotonia associated with caveolin-3 mutation. *Muscle Nerve* 45(6):897–900
- Mancioppi V et al (2023) A new mutation in the gene in two siblings with congenital generalized lipodystrophy type 4: case reports and review of the literature. *Front Endocrinol* 14:1212729
- Liu L, Pilch PF (2008) A critical role of cavin (polymerase I and transcript release factor) in caveolae formation and organization. *J Biol Chem* 283(7):4314–4322
- Liu L (2020) Lessons from cavin-1 deficiency. *Biochem Soc Trans* 48(1):147–154
- Betz RC et al (2001) Mutations in CAV3 cause mechanical hyperirritability of skeletal muscle in rippling muscle disease. *Nat Genet* 28(3):218–219
- Rajab A et al (2010) Fatal cardiac arrhythmia and long-QT syndrome in a new form of congenital generalized lipodystrophy with muscle rippling (CGL4) due to PTRF-CAVIN mutations. *PLoS Genet* 6(3):e1000874
- Lo HP et al (2011) Mosaic caveolin-3 expression in acquired rippling muscle disease without evidence of myasthenia gravis or acetylcholine receptor autoantibodies. *Neuromuscul Disord* 21(3):194–203
- Schoser B et al (2009) Immune-mediated rippling muscle disease with myasthenia gravis: a report of seven patients with long-term follow-up in two. *Neuromuscul Disord* 19(3):223–228
- Liewluck T, Goodman BP, Milone M (2012) Electrically active immune-mediated rippling muscle disease preceding breast cancer. *Neurologist* 18(3):155–158
- Dubey D et al (2022) Identification of caveolae-associated protein 4 autoantibodies as a biomarker of immune-mediated rippling muscle disease in adults. *JAMA Neurol* 79(8):808–816
- Ansevin CF, Agamanolis DP (1996) Rippling muscles and myasthenia gravis with rippling muscles. *Arch Neurol* 53(2):197–199
- Bettini M et al (2016) Immune-mediated rippling muscle disease and myasthenia gravis. *J Neuroimmunol* 299:59–61
- Kikuchi T et al (2005) Behavior of caveolae and caveolin-3 during the development of myocyte hypertrophy. *J Cardiovasc Pharmacol* 45(3):204–210
- Galbiati F et al (2001) Caveolin-3 null mice show a loss of caveolae, changes in the microdomain distribution of the dystrophin-glycoprotein complex, and T-tubule abnormalities. *J Biol Chem* 276(24):21425–21433
- Lo HP et al (2021) Cavin4 interacts with Bin1 to promote T-tubule formation and stability in developing skeletal muscle. *J Cell Biol* 220(12):e201905065
- Bastiani M et al (2009) MURC/Cavin-4 and cavin family members form tissue-specific caveolar complexes. *J Cell Biol* 185(7):1259–1273
- Parton RG, del Pozo MA (2013) Caveolae as plasma membrane sensors, protectors and organizers. *Nat Rev Mol Cell Biol* 14(2):98–112
- Lo HP et al (2015) The caveolin-cavin system plays a conserved and critical role in mechanoprotection of skeletal muscle. *J Cell Biol* 210(5):833–849
- Malette J et al (2019) MURC/CAVIN-4 facilitates store-operated calcium entry in neonatal cardiomyocytes. *Biochim Biophys Acta Mol Cell Res* 1866(8):1249–1259
- Seto N et al. (2020) Neutrophil dysregulation is pathogenic in idiopathic inflammatory myopathies. *JCI Insight* 5(3)
- Consortium, G.T. (2013) The genotype-tissue expression (GTEx) project. *Nat Genet* 45(6):580–585
- Dobin A et al (2013) STAR: ultrafast universal RNA-seq aligner. *Bioinformatics* 29(1):15–21
- Liao Y, Smyth GK, Shi W (2013) The Subread aligner: fast, accurate and scalable read mapping by seed-and-vote. *Nucleic Acids Res* 41(10):e108
- Robinson MD, McCarthy DJ, Smyth GK (2010) edgeR: a Bioconductor package for differential expression analysis of digital gene expression data. *Bioinformatics* 26(1):139–140
- Gene Ontology C et al. (2023) The gene ontology knowledgebase in 2023. *Genetics* 224(1)
- Ashburner M et al (2000) Gene ontology: tool for the unification of biology. The gene ontology consortium. *Nat Genet* 25(1):25–29
- Catteruccia M et al (2009) Rippling muscle disease and cardiomyopathy associated with a mutation in the CAV3 gene. *Neuromuscul Disord* 19(11):779–783
- Nicot AS et al (2007) Mutations in amphiphysin 2 (BIN1) disrupt interaction with dynamin 2 and cause autosomal recessive centronuclear myopathy. *Nat Genet* 39(9):1134–1139
- Shishmarev D (2020) Excitation-contraction coupling in skeletal muscle: recent progress and unanswered questions. *Biophys Rev* 12(1):143–153
- Bannister RA (2016) Bridging the myoplasmic gap II: more recent advances in skeletal muscle excitation-contraction coupling. *J Exp Biol* 219(Pt 2):175–182
- De Genst E et al (2022) Blocking phospholamban with VHH intrabodies enhances contractility and relaxation in heart failure. *Nat Commun* 13(1):3018
- Kranias EG, Hajjar RJ (2012) Modulation of cardiac contractility by the phospholamban/SERCA2a regulome. *Circ Res* 110(12):1646–1660
- Rubenstein AB et al (2020) Single-cell transcriptional profiles in human skeletal muscle. *Sci Rep* 10(1):229
- Pinal-Fernandez I et al (2019) Identification of distinctive interferon gene signatures in different types of myositis. *Neurology* 93(12):e1193–e1204
- Greenberg SA et al (2012) Relationship between disease activity and type 1 interferon- and other cytokine-inducible gene expression in blood in dermatomyositis and polymyositis. *Genes Immun* 13(3):207–213
- Pinal-Fernandez I et al (2023) Transcriptomic profiling reveals distinct subsets of immune checkpoint inhibitor induced myositis. *Ann Rheum Dis* 82(6):829–836
- Kistner TM, Pedersen BK, Lieberman DE (2022) Interleukin 6 as an energy allocator in muscle tissue. *Nat Metab* 4(2):170–179
- Song Q et al (2004) Overexpression of phospholamban in slow-twitch skeletal muscle is associated with depressed contractile function and muscle remodeling. *Faseb j* 18(9):974–976
- Fajardo VA et al (2015) Phospholamban overexpression in mice causes a centronuclear myopathy-like phenotype. *Dis Model Mech* 8(8):999–1009

55. Hagemann D, Xiao RP (2002) Dual site phospholamban phosphorylation and its physiological relevance in the heart. *Trends Cardiovasc Med* 12(2):51–56
56. Asahi M et al (2002) Sarcoplipin inhibits polymerization of phospholamban to induce superinhibition of sarco(endo)plasmic reticulum Ca²⁺-ATPases (SERCA_s). *J Biol Chem* 277(30):26725–26728
57. Naito D et al (2015) The coiled-coil domain of MURC/cavin-4 is involved in membrane trafficking of caveolin-3 in cardiomyocytes. *Am J Physiol Heart Circ Physiol* 309(12):H2127–H2136
58. Nakamori M et al (2017) Aberrant myokine signaling in congenital myotonic dystrophy. *Cell Rep* 21(5):1240–1252
59. Nath S (2025). <https://BioRender.com/k43m474>

Publisher's Note

Springer Nature remains neutral with regard to jurisdictional claims in published maps and institutional affiliations.